Effects of Mixing on Electrical Properties of Carbon Nanofiber and Polymer Composites

Sungho Lee, Young-Pyo Jeon

Center for Advanced Engineering Fibers and Films, Clemson University, Clemson, South Carolina 29634

Received 1 October 2008; accepted 6 March 2009
DOI 10.1002/app.30381
Published online 1 May 2009 in Wiley InterScience (www.interscience.wiley.com).

ABSTRACT: We examined electrical properties of composites of carbon nanofibers (CNFs)/linear low-density polyethylene (LLDPE) in the range of mixing time. An addition of CNFs into LLDPE led to a decrease of electrical resistivity, and the large amounts of CNFs were required to reach the electrical percolation threshold for the longer mixing time. For the research of these phenomena, we examined the effects of mixing time on the size (length) and spatial distributions of CNFs in the composites. SEM micrographs revealed the size reduction of CNFs in a series of mixing times, although the spatial dispersion of CNFs became more uniform at longer mixing time. To describe the reduction of CNFs theoretically, we hypothesize the size distribution of CNFs obeys a governing population balance kinetics based on an irreversible dissolution process. For the process, we proposed a size dependent breakage rate coefficient proportional to the size of CNFs. The model prediction for the time evolution of size distribution of CNFs has been validated with the experimental measurement showing good agreement. © 2009 Wiley Periodicals, Inc. J Appl Polym Sci 113: 2980–2987, 2009

Key words: nanocomposites; particle size distribution; modeling

INTRODUCTION

Polymeric composites with carbonaceous materials such as carbon black (CB),[1] carbon fiber (CF),[2,3] carbon nanofiber (CNF),[4–7] and carbon nanotubes (CNT)[8–10] are of interest in numerous engineering applications. Since carbonaceous materials have high electrical conductivity, polymeric composites with such materials can also be electrically conductive. In general, these materials are used for housing materials of electric devices to protect the devices from electromagnetic interference (EMI) or electrostatic discharge (ESD) phenomena.[1,3,7]

There has been a significant increase of using CNF because a smaller nano-scaled size and a higher aspect ratio (length to diameter) of CNF compared with CB or CF enable the composites to obtain desired electrical conductivity with smaller amount of materials.[10] It is evident that more conductive filler can result in higher electrical conductivity. However, the filler content should be low as possible for cost and efficiency. Composites with the higher filler content have low processibility, and furthermore, show poor mechanical performance due to the heterogeneity of composites.

The essential factor of composites to obtain the desired electrical conductivity is not only the filler content, but also the spatial dispersion of the conductive fillers.[4–6,8–10] Because of very strong van der Waals bonding force, CNFs are often tangled.[8] Therefore, when shear mixing is applied to a molten stage of polymer and CNF mixture at an extruder or a batch mixer, an appropriate shear force is required to untangle the CNF clusters and to distribute CNFs into the polymer.[4–6] However mixing has several distinct effects such as disentanglement of CNF agglomerates (or bundles), breakage of CNF bundles into smaller ones,[11] and fragmentation of individual CNFs into smaller (shorter) ones[12]; the terminology 'size (length)' in this study represents the size of individual CNFs not CNF bundles. Among many parameters that would have an effect on electrical conductivity such as the mixing force, shear rate, viscosity of matrix, etc, we are particularly interested in the size and dispersion of CNFs. Therefore, the rest of parameters will be standardized and fixed throughout the empirical and theoretical experiments.

The CNF network in the composites is very sensitive to the size distribution of CNFs, which is primarily depending upon the mixing process: longer CNFs are advantageous to construct the network. Hine et al.[5] incorporated CNF (*Pyrograf-III*™, *PR-19*) into polypropylene (PP) using a twin screw extruder. They observed a significant decrease of fiber length from 20 to 100 μm (from a manufacturer) to 2.53 ± 1.5 μm after mixing. To reduce this fiber breakage during fabrication of cnf/polymethyl

Correspondence to: Y.-P. Jeon (ypjeon@clemson.edu).

© 2009 Wiley Periodicals, Inc.

methacrylate (PMMA) composite during melt mixing, Jimenez and Jana[6] introduced a chaotic mixer, which provides lower shear stress compared to the conventional batch mixer, yielding longer fibers and larger agglomerates. Furthermore, they observed a percolation threshold ($\sim 10^6$ Ω cm) at ~2 wt % CNF content with chaotic mixing, whereas composites with internal mixing revealed a percolation threshold ($\sim 10^6$ Ω cm) at ~6 wt % CNF content.[6]

There are substantial experimental and theoretical researches, in estimating electrical conductivity of composites as a function of filler content. When conductive fillers are incorporated into polymer matrix, an abrupt decrease of volume resistivity, the inverse of the electrical conductivity, is observed at a percolation threshold, which can be defined as a critical concentration of conductive fillers. Percolation is observed when the filler forms a network to transfer electrons so that the composite system becomes electrically conductive. It is well known that electrons can be transferred by physical contacts of conductive fillers or by tunneling phenomena which allow electron migration through small gap between fillers.[1,2,4]

The objectives of the current work are to discuss effects of mixing on electrical properties of CNF/polymer composites and to reveal the evolution of the size distribution of CNFs. For that purpose, mixing time is the only variable parameter for the each set of experiment in the current study. In addition, we will introduce a fundamental framework to predict the CNF size distribution during the mixing process based on the distribution kinetics approach, and the calculation will be validated using the experimental size measurement of CNFs.

DISTRIBUTION KINETICS OF CNF FRAGMENTATION

The theory of particle fragmentation and aggregation has a wide range of engineering applications, and many mathematical efforts have been made for the particle fragmentation and aggregation processes. Hulburt and Katz[13] and Himmelblau and Bischoff[14] indicated that the fragmentation and aggregation equations can be applied to a wide range of particulate systems. McCoy and Madras[15] introduced continuous-distribution kinetics based on the population balance equation governing the behavior of the particle size distribution for simultaneous binary fragmentation and aggregation processes.

In general, particles can randomly aggregate and simultaneously fragment into smaller sizes that are distributed according to the force applied to the system. Particles fragment to yield random or parabolic size (length or mass) distributions according to the scission process such as random, mid-point, or chain-end scission.[14,16,17] Similar to the methods previously reported,[18] we hypothesize that the CNFs in the CNF/polymer composites fragment randomly into smaller sizes during the mixing process, and the process can be described by the irreversible fragmentation. We apply continuous-distribution kinetics to describe the evolution of CNF size distributions during the composite process. The size distribution of CNFs is defined as $p(\xi,t)d\xi$, describing the number of CNFs at time t in the size (length) interval ξ to $\xi+d\xi$. Similar to McCoy and Madras,[15] the binary irreversible fragmentation process can be expressed as an irreversible reaction-like process

$$\mathbf{P}(\xi') \xrightarrow{k_f(\xi)} \mathbf{P}(\xi) + \mathbf{P}(\xi' - \xi) \qquad \text{(A)}$$

where $k_f(\xi)$ is a breakage rate coefficient and $\mathbf{P}(\xi)$ represents a CNF with size ξ. Based on the continuous kinetics approach, the governing equation for the size distribution of CNFs is

$$\partial p(\xi,t)/\partial t = -k_f(\xi)p(\xi,t) + 2\int_0^{\xi} k_f(\xi')\, p(\xi',t)\Omega(\xi,\xi')\, d\xi' \qquad (1)$$

where $\Omega(\xi, \xi')$ is the breakage kernel for a CNF of length ξ' that fragments into products of length ξ and $\xi'-\xi$, and the factor 2 appears to provide appropriate stoichiometric coefficients for the total number of CNFs (zeroth moments). We apply the stoichiometric kernel proposed by McCoy and Wang[19] that is proportional to $\xi^m(\xi' - \xi)^m$.

$$\Omega(\xi,\xi') = \xi^m(\xi'-\xi)^m\Gamma(2m+2)/[\Gamma(m+2)^2(\xi')^{2m+1}] \qquad (2)$$

where the gamma function has the property, $\Gamma(n + 1) = n\Gamma(n) = n!$, if n is positive integer. When $m = 1$, the kernel has the parabolic form, $\Omega(\xi, \xi') = 6\xi(\xi' - \xi)/\xi'^3$, if $m \to \infty$, the kernel describes the midpoint fission, $\Omega(\xi, \xi') = \delta((\xi - \xi'/2)$, and at $m = 0$, the kernel corresponds to the random fission, $\Omega(\xi, \xi') = 1/\xi'$.[19] We will consider the breakage of CNF as a random fission process, and thus, the breakage kernel is $\Omega(\xi, \xi') = 1/\xi'$. We propose to use the size dependent breakage rate coefficient proportional to the length of CNFs as

$$k_f(\xi) = \kappa\xi^{\lambda} \qquad (3)$$

The general nth moments of the size distribution of CNFs are defined as

$$p^{(n)}(t) = \int p(\xi,t)\xi^n\, d\xi \qquad (4)$$

where the integration limits are determined by the domain of $p(\xi,t)$. From the definition, the total

number of and the total mass of CNFs are $p^{(0)}(t)$ and $p^{(1)}(t)$, respectively, and the number-average (M_n) and weight-average (M_w) of CNFs are $M_n = p^{\text{avg}}(t) = p^{(1)}(t)/p^{(0)}(t)$ and $M_w = p^{\text{avg2}}(t) = p^{(2)}(t)/p^{(1)}(t)$, respectively. The variance and polydispersity index in terms of the second moment are defined as $p^{\text{var}} = p^{(2)}/p^{(0)} - p^{\text{avg2}}$ and $p^{\text{pd}} = p^{(2)}p^{(0)}/p^{(1)2}$, providing further information for the character and shape of the distribution.

By applying the moment operation in eq. (4), eq. (1) yields

$$dp^{(n)}(t)/dt = -\kappa p^{(n+\lambda)}(t) + 2[1/(n+1)]\kappa p^{(n+\lambda)}(t) \tag{5}$$

We define new time variable, $d\theta = \kappa\, dt$, and the differential equations for the first three moments are

$$dp^{(0)}(\theta)/\, d\theta = p^{(\lambda)}(\theta) \tag{6}$$

$$dp^{(1)}(\theta)/d\theta = 0 \tag{7}$$

$$dp^{(2)}(\theta)/d\theta = -(1/3)p^{(\lambda+2)}(\theta) \tag{8}$$

Equation (7) indicates the first moment is constant satisfying the mass conservation. McCoy and Madras[15] defined a similarity solution for fragmentation-aggregation showing the Poisson function form as

$$p(\xi,t) = \{p^{(1)}(t)\lambda/[\beta^{2/\lambda}\Gamma(\alpha - 1 + 2/\lambda)]\}(\xi^{\lambda}/\beta)^{\alpha-1}\exp(-\xi^{\lambda}/\beta) \tag{9}$$

where α is constant ($\alpha = 1$ for random fission) and $\beta(t)$ is a function of time. The general nth moment for eq. (9) is

$$p^{(n)}(t) = p^{(1)}(t)\beta^{(n-1)/\lambda}\Gamma[\alpha - 1 + (n+1)/\lambda]/\Gamma(\alpha - 1 + 2/\lambda) \tag{10}$$

The number-average ($M_n = p^{(1)}/p^{(0)}$) of CNFs is $M_n = \beta^{1/\lambda}\,\Gamma(\alpha - 1 + 2/\lambda)\,/\,\Gamma(\alpha - 1 + 1/\lambda)$, which can be simplified as $M_n = \alpha\cdot\beta$ for $\lambda = 1$. By substituting eq. (10) into eq. (6) to (8), we have

$$d(\ln h_1)/d\theta = \beta(\alpha - 1 + 1/\lambda) \tag{11}$$

$$d(\ln p^{(1)}(\theta))/d\theta = 0 \tag{12}$$

$$d(\ln h_2)/d\theta = -\beta(\alpha - 1 + 3/\lambda)/3 \tag{13}$$

where

$$h_1 = \beta^{-1/\lambda}\Gamma(\alpha - 1 + 1/\lambda)/\Gamma(\alpha - 1 + 2/\lambda) \tag{14}$$

$$h_2 = \beta^{1/\lambda}\Gamma(\alpha - 1 + 3/\lambda)/\Gamma(\alpha - 1 + 2/\lambda) \tag{15}$$

Extracting eq. (11) with eq. (12) yields an expression for $\beta(\theta)$,

$$d\beta(\theta)/d\theta = -\lambda\beta^2(\alpha - 1 + 1/\lambda) \tag{16}$$

To obtain an expression α, we combine eqs. (11) and (13) applying eq. (12).

$$d\alpha/d\theta\; d\ln[\Gamma(\alpha - 1 + 1/\lambda)\Gamma(\alpha - 1 + 3/\lambda)/\Gamma(\alpha - 1 + 2/\lambda)^2]/d\alpha = 2\beta(\alpha - 1)/3 \tag{17}$$

For random fission ($\alpha = 1$), when we approximate the linear size dependence of the fission rate coefficient ($\lambda = 1$) for a range of CNF sizes, eq. (16) becomes $d\beta(\theta)/d\theta = -\beta^2$, yielding a simple expression as $\beta(\theta) = \beta_o\,/\,(1 + \beta_o\theta)$, where $\beta(0) = \beta_o$. Therefore the size distribution of CNFs is

$$p(\xi,t) = p^{(1)}(t)\exp(-\xi/\beta)/\beta^2 = p^{(0)}(t)\exp(-\xi/\beta)/\beta \tag{18}$$

Equation (18), a similarity solution for the random fragmentation process, has been derived by Ziff,[20] Peterson,[21] and Madras and McCoy.[22]

We now substitute the size distribution of CNF evaluated in eq. (18) into the moment expression defined in eqs. (6) and (7). From eq. (7), we obtain the first moment $p^{(1)}(\theta) = p_o^{(1)}$, which satisfies the mass conservation, and for random fission ($\alpha = 1$) with $\lambda = 1$, eq. (6) simply becomes $dp^{(0)}(\theta)/d\theta = p_o^{(1)}/\beta(\theta)$. Therefore, the total number of CNFs expressed as the zeroth moment is expressed as

$$p^{(0)}(\theta) = p_o^{(0)} + p_o^{(1)}(\theta/\beta_o + \theta^2/2) \tag{19}$$

EXPERIMENTAL

Carbon nanofibers (CNFs, *PR-24-PS*) provided by *Applied Sciences, Inc*. (Applied Science Inc., Cedarville, OH) were synthesized using the chemical decomposition of natural gas over iron-sulfide catalyst.[23] Diameter and length of CNFs were found to be 116 ± 46 nm and 1–60 μm, respectively. Entangled nature of as-received CNFs is pictured by scanning electron microscope (SEM) and presented in Figure 1 poly(ethylene-*co*-1-octene) (DOWLEX 2045 LLDPE, Dow Chemical) was used as the matrix for this study. The properties of the resin given by the manufacturer are density of 0.920 g/cm^3, melt flow index (MFI) of 1.0 g/10 min, DSC melting point of 122°C, and softening point of 108°C.

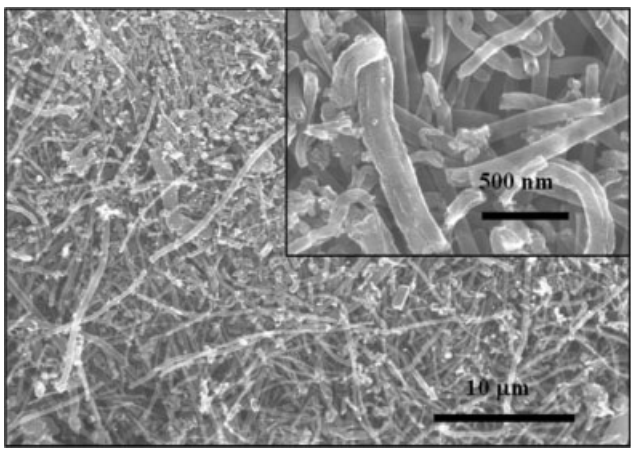

Figure 1 A SEM image of the as-received CNFs showing entangled nature.

Rheomix 600 mixer (Haake Inc.) was used for intensive mixing of pure LLDPE and various contents (1 – 20 wt %) of CNFs. Physically blended LLDPE and CNFs were fed into the device and mixed with various times (2, 6, and 18 min) under nitrogen atmosphere. Mixing conditions are standardized and fixed at 190°C with a screw rotating speed of 30 rpm throughout the experiments. Next, the compounded forms of pure LLDPE and nanocomposites were placed on a Carver laboratory press at 190°C. Before compacting, 2.8 MPa of pressure was applied during 5 min preheating to soften the materials. Subsequently, 5.5 MPa of pressure was applied for 3 min, and pressed samples were air-cooled down to ambient conditions for 10 min.

The electrical resistivity was measured by a Megohmmeter ACL 800 digital ohmmeter at 25°C. In addition, we have experimentally measured the size distribution of CNFs before and after the mixing process, which is used to validate the theoretical predictions. For the study of CNF dispersion, composite samples containing 1 wt % CNFs were observed by using Olympus BX-60 optical microscope, and micrographs of the cryofractured cross-section of the composites were taken by Hitachi FE S-4300 SEM. For the size measurement of CNFs, the polymer matrices in the nanocomposite samples were decomposed by Pyris 1 Perkin-Elmer thermo gravimetric analysis (TGA) at 600°C under nitrogen. To take the SEM images, the residues from TGA experiment are dispersed in acetone by sonication for 10 min and dispensed into the formvar/carbon film-supported copper grid for drying. The experimental size distributions of CNFs were constructed by a binning operation through image analysis of SEM images, which divides the total CNF size (length) range into intervals bins and then counts the number of CNFs in each bin. The frequency size distribution is normalized from 0 to 1 by its maximum frequency, and then is plotted versus size of CNFs on normal coordinates, yielding an exponential distribution (Fig. 6).

RESULTS AND DISCUSSION

Figure 2 represents the volume resistivity of the CNF/LLDPE composites as a function of CNF contents in the range of mixing time (2, 6, and 18 minutes). For composites mixed for 2 min, the volume resistivity does not change significantly up to 5 wt % CNF content, *which implies CNF networks has not been constructed yet*. A volume resistivity of composites with 7 wt % CNF, however, dropped over five orders of magnitude (down to 3.3×10^5 Ω cm), indicating electrical network construction among CNFs in the composites. Based on our resistivity measurement for the CNF/LLDPE composite mixed for 2 min, 7 wt % CNF content is the electrical percolation threshold at which the composite shows a distinct electrically conductive characteristic. As shown in Figure 2, the nonlinear volume resistivity of the composites is inversely proportional to CNF content, and reaches its minimum, 3.3×10^2 Ω cm, at 20 wt % of CNFs.

Compared to the composite mixed for 2 min, the composite mixed for 18 min showed a significantly high volume resistivity (1.4×10^{10} Ω cm) at 7 wt % CNF content. For the composite mixed for 18 min, a significant decrease of volume resistivity (1.4×10^7 Ω cm), which is three orders of magnitude higher than that of the composite mixed for 2 min (6.5×10^3 Ω cm), was observed as the CNF content increases from 7 wt % to 10 wt %. As expected, the

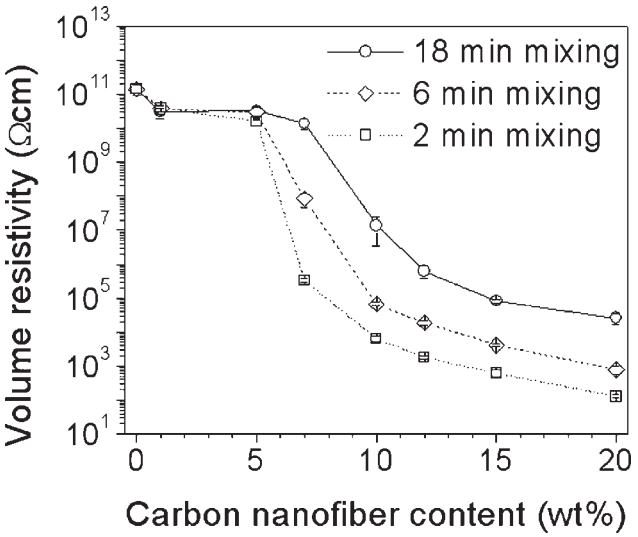

Figure 2 The effect of CNF content and mixing time on the volume resistivity of CNF/LLDPE composites: symbols (□ - 2 min, ◇ - 6 min, and ○ - 18 min mixing) representing experimental data are connected by trend lines.

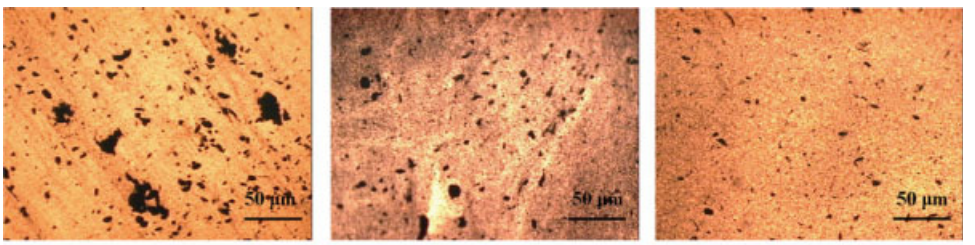

Figure 3 Optical micrographs of composites containing 1 wt % CNFs mixed for (a) 2 min, (b) 6 min, and (c) 18 min. [Color figure can be viewed in the online issue, which is available at www.interscience.wiley.com.]

volume resistivity of the composite mixed for 6 min is located between the volume resistivities of the composite mixed for 2 and 18 min, showing intermediate behavior between them (Fig. 2).

According to percolation theory,[24] the evolution of conductivity beyond the percolation threshold can be described as

$$\sigma \propto (p - p_c)^n \tag{20}$$

where σ, p, and n are the conductivity, volume fraction of CNF, and the critical exponent, respectively, and the subscript c represents critical value at the percolation threshold. Based on the volume resistivity evolution illustrated in Figure 2, the critical exponent, n, is calculated to be 2.4, 2.1, and 2.0 for the composites mixed for 2, 6, and 18 min, respectively. The composite with the larger critical exponent shows more drastic resistivity dropping-off, electrical conductivity kicking-in. Experimentally, the critical exponent in CNF/PP composites reported by Andrade et al. is 1.9,[25] which is compatible with our measurement.

An optical microscope was used to observe dispersion of CNF agglomerates (1 wt %) in composites after mixing. As indicated in Figure 3(a–c), as mixing time increases from 2 to 18 min, large agglomerates in the composite gradually disappear showing more uniform distribution of CNFs, although individual fibers become shorter in length.

Jimenez and Jana measured the size of agglomerates in CNF/PMMA composites for both chaotic and conventional batch mixing, and observed larger agglomerates in the chaotic mixing with mild shear conditions, which corresponds to the shorter mixing time for our experiment.[6] It is inferred that longer mixing time providing more shear stress led to increase of disentanglement of CNF agglomerates. SEM micrographs of cryofractured cross-section of composites containing 7 wt % of CNF with 2, 6, and 18 min mixing are listed in Figure 4 in accordance with the previous report[6]; a distribution dominance at an initial stage of mixing in Figure 4(a,b) and a size reduction dominance at a final stage of mixing in Figure 4(c). Therefore composites with longer mixing time showed more uniform CNF distributions and smaller CNF agglomerates in number and size, showing clear effects of mixing time on the spatial distribution of CNFs and the size distribution of CNFs and its agglomerates.

To measure the size (length) of individual CNF, SEM micrography was performed for as-received CNFs and the residual CNFs after TGA of composites containing 7 wt % CNF with 2, 6, and 18 min mixing. The inset of Figure 5 shows a SEM reference image for us to measure the size (length) of CNFs by the image analysis. More than 30 SEM images were taken and 400 CNFs were measured for each condition (before mixing, and 2, 6, and 18 min mixing samples). Figure 5 displays frequency distributions of CNF length before and after mixing. The distribution in Figure 5 is a modified Poisson distribution, one of the representative unimodal distributions, with the tail-end behavior. We have already defined the general nth and 0th moments in eqs. (10) and (19), therefore, statistical properties such as mean and variance can be theoretically defined and measured. As-received CNFs have a length of up to 60 μm, and a broader length distribution was observed compared to CNFs in composites. As shown in Figure 5, as mixing time increased from 2 to 6 min, long fibers disappeared resulting in a higher frequency of short fibers and a narrower size distribution of CNFs. In addition, the medium and variances for the size distribution of CNFs experimentally measured; (a) 0 min: 5.69 $\pm$ 7.46 mm, (b) 2 min: 3.85 $\pm$ 22.61 mm, (c) 6 min: 3.29 $\pm$ 12.21 mm, and (d) 18 min: 3.00 $\pm$ 10.05 mm. Therefore, it is clear that mixing led to the breakage of CNFs. Because of the lower aspect ratio, the composite mixed for 6 min requires a larger amount of CNFs to reach the electrical percolation, although it shows more uniform dispersion than the composite mixed for 2 min.

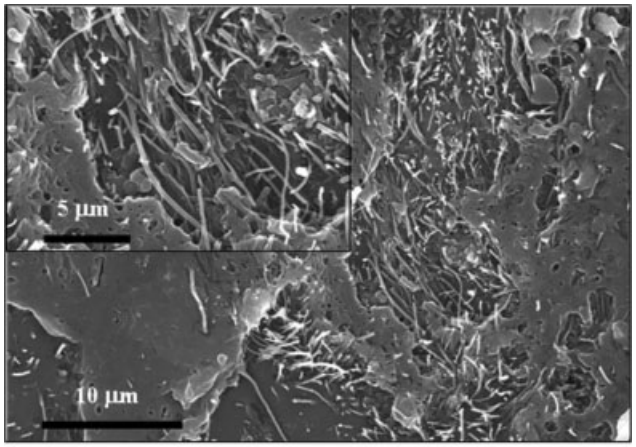

(a) 2 minute mixing composite.

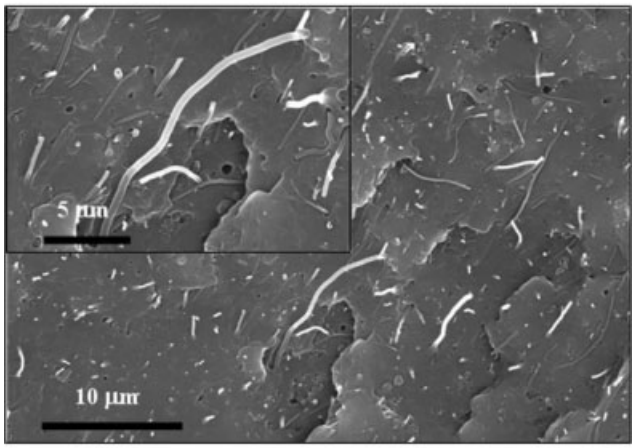

(b) 6 minute mixing composite.

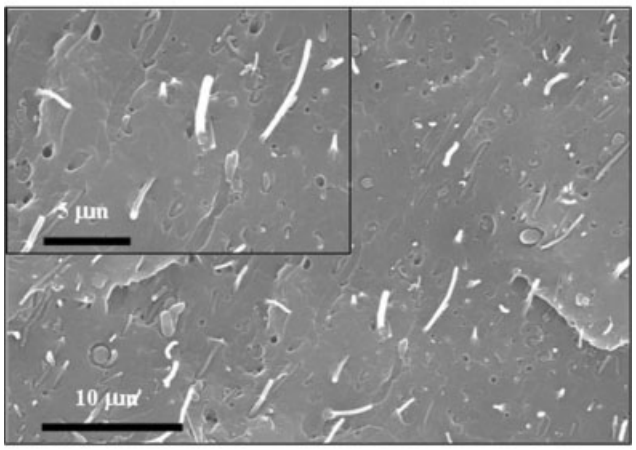

(c) 18 minute mixing composite.

Figure 4 SEM micrographs of composites containing 7 wt % CNFs mixed for (a) 2 min, (b) 6 min, and (c) 18 min.

In Figure 3(c), an optical micrograph of 18 min mixing composite, we observed that CNF agglomerates become smaller compared to 2 min [Fig. 3(a)] and 6 min [Fig. 3(b)] mixing composites, and the smaller agglomerates are dispersed through the composite as mixing time increase. The effects of mixing time on CNF and its bundle sizes are clearly captured in Figure 4(a–c); as mixing time increase, CNF aggregates are disentangled and individual CNFs are dispersed through the composite experiencing the breakage process. The size (length) distributions of CNFs in the composites mixed for 6 and 18 min show no significant variation in Figure 5. However, the volume resistivity showed a clear difference between the ranges of mixing time (Fig. 2). These imply that after 6 min mixing, the degree of fiber distribution become a more dominant factor affecting the volume resistivity (electrical conductivity) of the composites than the fiber size (breakage or length).

As mentioned, the volume resistivity dropping-off can be observed at the percolation threshold of the CNF network, and well distributed longer CNFs in the composite can form the filler network earlier than poorly distributed shorter CNFs. In this sense, the optimum mixing would be the one dispersing CNFs uniformly with minimal amount of the breakage in CNFs.

We have observed the clear effect of mixing on the volume resistivity (Fig. 2). The volume resistivity as a function of the mixing time and the CNF content were experimentally examined. In addition, we have also found the size change of CNFs during the mixing process (Fig. 5). It is evident that CNFs break down into smaller sizes as a result of mixing. Based on the random fragmentation of CNFs, we have evaluated the size distribution of CNFs as a function of mixing time, eq. (18). The evolution of the size distribution during the mixing process is theoretically calculated and plotted with the experimental measurement (Fig. 6). In Figure 6, the predictions of eqs. (18) and (19) and the experimental measurements of the size distributions of CNFs are normalized from 0 to 1 with their maximum values and plotted as solid lines (predictions) and symbols

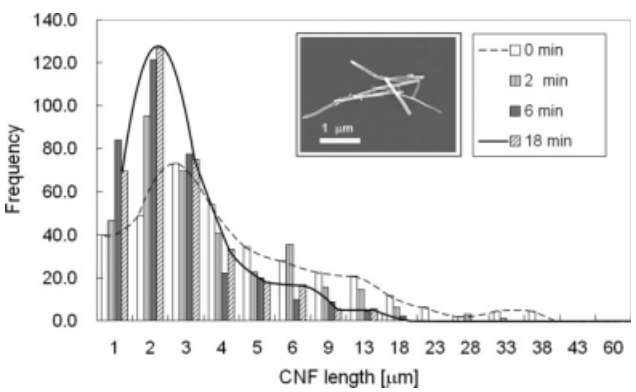

Figure 5 Histograms of CNF length distribution in composites containing 7 wt % CNFs before and after mixing. The inset image is a representative SEM micrograph of residual CNFs after decomposing.

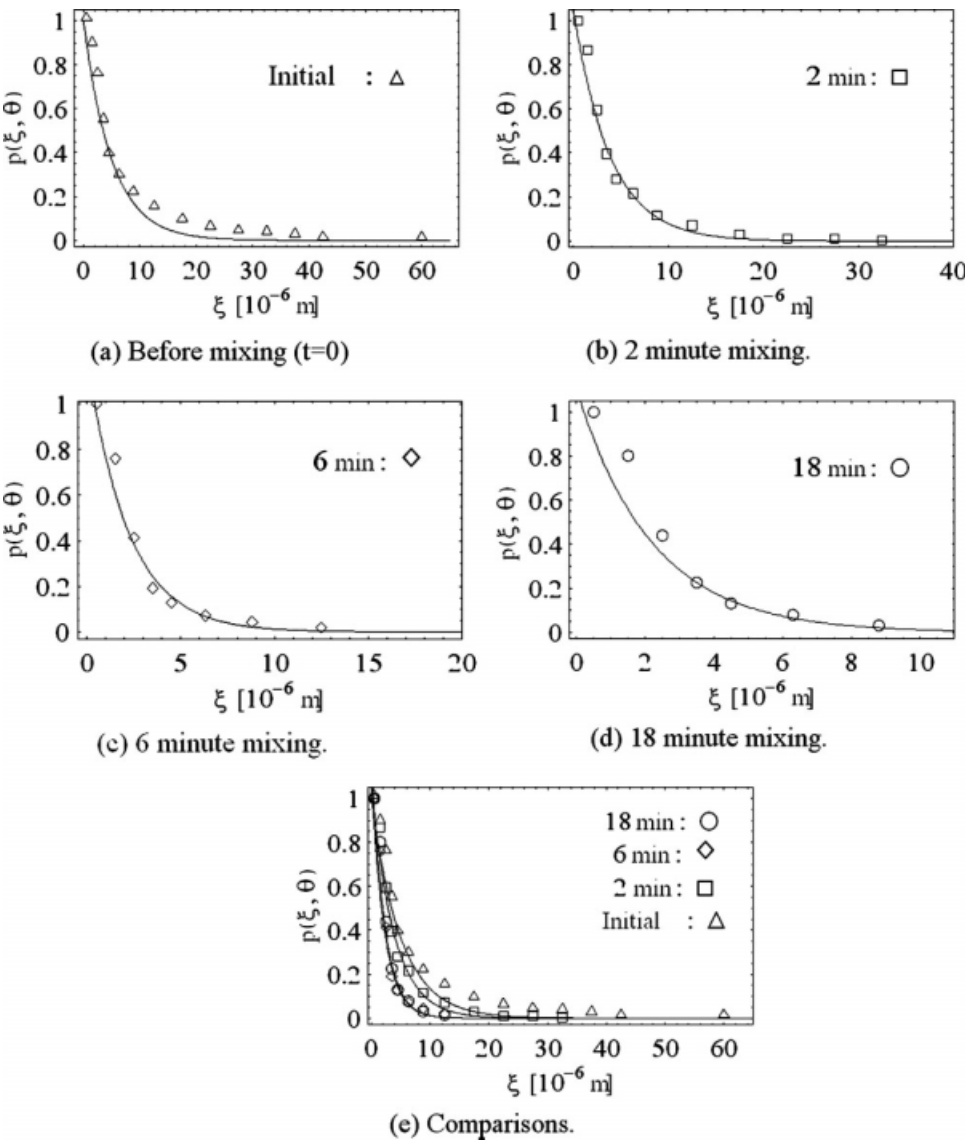

Figure 6 The evolution of the size distribution of CNFs in the composites of 7 wt % CNFs when CNFs undergo random fission: parameters for the model predictions are $p_o^{(0)} = 106$, $\kappa = 0.2$, and $\beta_o = 5$, respectively.

(experiments), respectively, showing good agreements. By the validation of the model prediction of CNF size distributions, we have clearly demonstrated the effect of mixing on CNF size (length).

CONCLUSION

We have investigated the effects of mixing on electrical properties of CNF/LLDPE composites. To examine the mixing effects, the volume resistivity of the composite was experimentally measured in the range of mixing time and CNF contents. Depending upon the composite conditions, the electrical conductivity kicking-in, which is expressed as the sudden volume resistivity dropping-off, was observed at the percolation threshold, a point of CNF network construction.

For CNF/polymer composites, if one can disperse the CNFs without the breakage process, so that the CNF network is constructed with the least amount of CNFs, this will be the most efficient composite process. Such process, however, may not be realistic, because the CNF network construction in the composite is a trade-off between dispersion of and size (length) of CNFs, which are in a reciprocal relationship: longer mixing is preferable for uniform distribution of CNFs, whereas shorter mixing is favorable to prevent the breakage of CNFs.

We have investigated the effect of mixing time and CNF contents for the spatial dispersion of and temporal size distribution of CNFs. The effect of mixing time on the spatial dispersion of CNFs in the composites is experimentally investigated by using SEM micrograph, and it revealed the spatial

dispersion of CNFs became uniform for a longer mixing. We have also researched the temporal size distribution of CNFs in the composites. The size distribution of CNFs has been theoretically developed using population balance kinetics based on the irreversible random breakage process. The hypothesis that the size distribution of CNFs obeys a population balance equation reasonably describes the fiber breakage process. The moment method is also applied to the size distribution to obtain the total number of CNFs as a function of mixing time. The decreasing size distributions of CNFs in the range of mixing time were experimentally measured, and the theoretical prediction has been validated with the measurement.

Because the longer mixing make the average CNF size smaller, the composite mixed for 18 min required more amount of CNFs to reach the percolation threshold of the CNF network than the composite mixed for 2 min. This indicates a reciprocal relationship between the spatial dispersion of and temporal size distribution of CNFs, which are essential to CNF network construction in the composite. Therefore, the mixing time with respect to the CNF contents should be optimized to obtain CNF/polymer composites with desired electrical properties. As we have concluded, an ideal mixing would be the one dispersing CNFs without breakage in length. The fiber breakage, however, cannot be avoided due to the nature of mixing which leads to shear stress on CNFs. Among the mixing time we have examined, 2 min mixing provided the best electrical properties of resulting composites, however, further efforts should be made to obtain the optimum mixing time.

The purpose of this article was to examine the effects of mixing on electrical properties of CNF/polymer composites. The current article shows clear effects of mixing time and CNF contents on the volume resistivity, the inverse of the electrical conductivity, of the composite through the CNF network construction. The theoretical approach on this article was focused only on the size distribution of CNFs as a function of mixing time, and the model in its present state is not able to describe spatial dispersion of CNFs. At present, no single model quantitatively describes the spatial dispersion of and temporal size distribution of CNFs in the composites. To describe the spatial dispersion of CNFs associated with the networking behavior in the composites, more complex model should be considered.

References

1. Foulger, S. H. J Appl Polym Sci 1999, 72, 1573.
2. Vilcakova, J.; Saha, P.; Quadrat, O. Eur Polym J 2002, 38, 2343.
3. Jou, W. S.; Wu, T. L.; Chiu, S. K.; Cheng, W. H. J Electron Mater 2002, 31, 178.
4. Finegan, I. C.; Tibbetts, G. G. J Mater Res 2001, 16, 1668.
5. Hine, P.; Broome, V.; Ward, I. Polymer 2005, 46, 10936.
6. Jimenez, G. A.; Jana, S. C. Compos A 2006, 38, 983.
7. Yang, S.; Lozano, K.; Lomeli, A.; Foltz, H. D.; Jones, R. Compos A 2005, 36, 691.
8. Potschke, P.; Bhattacharyya, A. R.; Jake, A. Eur Polym J 2004, 40, 137.
9. Du, F.; Scogna, R. C.; Zhou, W.; Brand, S.; Fischer, J. E.; Winey, J. E. Macromolecules 2004, 37, 9048.
10. Thostenson, E. T.; Li, C.; Chou, T. W. Compos Sci Technol 2005, 65, 491.
11. Li, C.; Thostenson, E. T.; Chou, T. W. Compos Sci Technol 2008, 68, 1227.
12. Li, J.; Ma, P. C.; Chow, W. S.; To, C. K.; Tang, B. Z.; Kim, J. K. Adv Funct Mater 2007, 17, 3207.
13. Hulburt, H. M.; Katz, S. Chem Eng Sci 1964, 19, 555.
14. Himmelblau, D. M.; Bischoff, K. B.Process Analysis and Simulation: deterministic Systems; Wiley: New York, USA, 1968.
15. Mccoy, B. J.; Madras, G. J Colloid Interface Sci 1998, 201, 200.
16. Price, G. J.; Smith, P. F. Polym Int 1991, 24, 159.
17. Madras, G.; Smith, J. M.; Mccoy, B. J. Polym Degrad Stab 1996, 52, 349.
18. Jeon, Y.-P.; Mccoy, B. J. Phys Rev E 2005, 72, 037104–1.
19. Mccoy, B. J.; Wang, M. Chem Eng Sci 1994, 49, 3773.
20. Ziff, R. M. J Phys A: Math Gen 1991, 24, 2821.
21. Peterson, T. W. Aerosol Sci Technol 1986, 5, 93.
22. Madras, G.; Mccoy, B. J. AIChE J 1998, 44, 647.
23. Tibbetts, G. G.; Lake, M. L.; Strong, K. L.; Rice, B. P. Compos Sci Technol 2007, 67, 1709.
24. Stauffer, D.; Aharony, A.Introduction to percolation theory; Taylor & Francis Ltd.: London, England, 1992.
25. Andrade, J. S. Jr., ; Auto, A. M.; Kobayashi, Y.; Shibusa, Y.; Shirane, K. Phys A 1998, 248, 227.